World Academy of Science, Engineering and Technology
International Journal of Civil and Environmental Engineering
Vol:9, No:7, 2015

Risk of Plastic Shrinkage Cracking in Recycled Aggregate Concrete

M. Eckert, M. Oliveira

***Abstract*—**The intensive use of natural aggregates, near cities and towns, associated to the increase of the global population, leads to its depletion and increases the transport distances. The uncontrolled deposition of construction and demolition waste in landfills and city outskirts, causes pollution and takes up space. The use of recycled aggregates in concrete preparation would contribute to mitigate the problem. However, it arises the problem that the high water absorption of recycled aggregate decreases the bleeding rate of concrete, and when this gets lower than the evaporation rate, plastic shrinkage cracking occurs. This phenomenon can be particularly problematic in hot and windy curing environments. Cracking facilitates the flow of liquid and gas into concrete which attacks the reinforcement and degrades the concrete. These factors reduce the durability of concrete structures and consequently the lifetime of buildings. A ring test was used, cured in a wind tunnel, to evaluate the plastic shrinkage cracking sensitivity of recycled aggregate concrete, in order to implement preventive means to control this phenomenon. The role of several aggregate properties on the concrete segregation and cracking mechanisms were also discussed.

***Keywords*—** Recycled Aggregate, Plastic Shrinkage Cracking; Wind Tunnel, Durability.

I. Introduction

PLASTIC shrinkage cracking (PShC) occurs in the first hours after casting when the concrete stiffness begins to develop. When the evaporation rate is faster than the bleeding rate, the concrete surface dries and the water is removed from the pores. Evaporation causes capillary stress when the concrete microstructure stops to be liquid, leading to cracks because the tensile strength is very low at this stage [1]. PShC typically occurs in thin concrete members with large surface areas, when exposed to hot, dry and windy environmental conditions responsible for high evaporation rates. The cracks weaken the concrete structure and allow the access of water and gases which transports aggressive species into the concrete. This leads to deterioration of concrete due to carbonation, chlorides, and corrosion of the reinforcement, reducing significantly the service life of a concrete structures [2]. Recycled aggregates (RA) have a high water absorption capacity. It is therefore expected a reduction of bleeding water which makes concrete more prone to PShC. It is therefore important to evaluate and quantify PShC in order to prevent or mitigate it. This paper reports a study of the role of RA aggregates on the PShC properties of concrete prepared thereof, based on the properties of the aggregates and on a comparison with concrete prepared with natural aggregates (NA).

M. Eckert is with the Civil Engineering Department, University of Algarve, Faro 8005-139 Faro, Portugal (phone: 289 800 100; fax: 289 800 061; e-mail: mabaec@yahoo.de).

M. Oliveira is the Director of the Civil Engineering Department, Head of Construction Materials Laboratory, University of Algarve, Faro 8005-139 Faro, Portugal (phone: 289 800 100; fax: 289 800 061; e-mail: molivei@ualg.pt).

II. State-of-the-Art

If shrinkage is restrained, residual tensile stress is generated and when this exceeds the tensile strength, concrete cracks [3]. PShC can be attributed to four driving forces [4]: I - Capillary stresses near the surface. On drying, a meniscus is formed in the capillaries causing tensile stress in the capillary water. This tensile stress must be balanced by compressive stress in the surrounding solid, leading to plastic shrinkage. Evaporation reduces the humidity state of concrete, leading to capillary stress raise as the pore radius decreases. The maximum capillary tension is reached immediately before the pores are completely emptied. This rupture relieves the stress level [5], [6]. II- Differential settlement. In the fresh state the shrinkage is not isotropic and segregation occurs. When the gravitational displacements are restricted by reinforcing steel or at locations with sudden change in cross-sectional thickness, cracking occurs [7]. III- Differential thermal expansion in which a temperature gradient develops from the element core to the surface [8], [9]. IV- Autogenous shrinkage in the plastic phase. Autogenous shrinkage has been defined as "the bulk deformation of a closed, isothermal, cementitious material not subjected to external forces" [10]. This deformation is caused by chemical shrinkage [11], [12], and self-dessication in which the capillary stress is built up by the water consumption of the hydration reactions [13]. Self-desiccation only occurs in low w/c ratio concrete and consequently in ordinary concrete autogenous shrinkage is not a concern. This four factors act simultaneously and depend on the mix composition, setting times and the environmental curing conditions, turning PShC in a very complex phenomena.

PShC can be located in the concrete microstructure evolution [14]. Before initial setting time the evaporation rate gets faster than the bleeding rate. Capillary pressure raises until the voids get completely empty and air enters, dropping the pressure to zero. When the initial setting time is reached bleeding stops. The first cracks can be observed after the initial setting time [15]. At this stage an unidirectional mineral percolation threshold will built up [13], [16], the concrete starts to stiff and the shrinkage strain turns isotropic [17]. The PShC is proportional to the amount of water evaporated before the initial setting time [18]. Between the initial and final

setting time the plastic shrinkage continues and the crack width increases progressively. When the final setting time is reached a 3 dimensional mineral percolation threshold is built up [13], [16], and PShC stops [14].

Relative humidity (RH) is the most influent environmental factor which aggravates PShC [7]. RH is followed by air velocity and temperature [7]. To prevent PShC several methods have been investigated and used. It is recommended that the water evaporation should be reduced or compensated when the evaporation rate is higher than 1 Kg/m² per hour [7]. This can be done by spraying water or curing compounds or applying protective cover sheets on the concrete surface [19]. Shrinkage reducing admixtures have also been tested and it was proven that they reduce PShC by lowering the water surface tension and consequently the capillary stress [19], [20], [21]. Internal curing by saturated lightweight aggregates or superabsorbent polymers also reduces PShC [22]. Several types of fibers were investigated to reduce PShC and it was found that they reduce the crack width and the crack area but cracking is not avoided [23], [24]. The cracking area increases with the w/c ratio and also with the amount of binder, due to a later setting and a bigger amount of evaporated water [2]. Superplasticizer and curing agents improve the ability to resist PShC [25]. The cracking time is proportional to the setting time but the cracking width or area is inversely proportional to it, due to a higher amount of evaporated water before the initial setting time. Thus a set accelerator reduces the crack area and set retarder increases the crack area [19], [26]. Settlement increases with the bleeding water which in turn increases with the setting time. Shrinkage reducing admixtures have a beneficial effect on settlement because these admixtures reduce plastic shrinkage in the vertical direction as well as in the horizontal direction.

III. Characterization of Aggregates

The aggregates were provided by the recycling plant "Multi-Triagem" which collects and manages the C&DW from the SW of the Algarve, Portugal. The primary reduction of the rubble was made with a shear. Then a primary and secondary crushing was performed using a portable Impact Crusher, fitted with two hammers and a magnetic separator. Finally the aggregates were sieved to obtain the desired fraction. In this work 4 types of coarse aggregates, labeled RA1, RA2, NA1 and NA2 and two types of fine aggregates, labeled RS and CS, were analyzed. The NA and CS are of crushed limestone and RS is fine limestone river sand.

A. Aggregate Test Program

Constituents of the coarse RA - examined according to NP EN 933-11 [27], in which RA are grouped in the following categories:

- ⇒ Rc: concrete, concrete products, masonry concrete blocks;
- ⇒ Ru: unbounded aggregates, natural stone, treated aggregates with hydraulic binder;
- ⇒ Rb: ceramic elements (e.g. bricks, roof tiles, etc), not floating cellular concrete and masonry blocks;
- ⇒ Ra: bituminous materials;
- ⇒ Rg: glass;
- ⇒ X: cohesive materials (soil, clay, etc.), metals, wood, plastic, rubber, stucco;
- ⇒ FL: floating materials.

Particle size distribution - according to NP EN 933-1 [28]. Size class - according to NP EN 12620 [29]. Mytilene blue - according to NP EN 933-9 [30]. Sand equivalent according to NP EN 933-8 [31]. Shape index - according to NP EN 933-4 [32]. Wet and dry specific densities according to da NP EN 1097-6 [33]. Water absorption - the pycnometer method was used according to NP EN 1097-6 [33]. Los-Angeles coefficient - according to NP EN 1097-2 [33]. Drying shrinkage - according to EN NP 1367-4 [34].

A reference mix was prepared using the four NA and 2 mixes with RA. In this mixes the coarse NA was replaced by each type of RA and the fine NA was kept. It was necessary to add extra water, equivalent to the aggregate absorption capacity, to enable compaction of the specimens.

Mass stability - was obtained by measuring the mass change in one drying and wetting cycle described in the EN NP 1367-4 [34].

B. Aggregate Test Results and Discussion

Constituent test (Table I): The major constituent of RA is old concrete or mortar, followed by ceramic materials and natural stone. This is in agreement with the literature [35], [36]. where the natural stones are included in the concrete category. The crushing process might lead to a separation of natural stones from mortar. The fraction of other constituents is very low.

Sieve analysis: According to Table II RA shows generally higher content in fines than the NA. RA2 shows significantly more fines than RA1. These differences may be attributed to the nature of its constituents. However, Fig. 1 shows that both RA give rise to a compact size distribution near to reference grades.

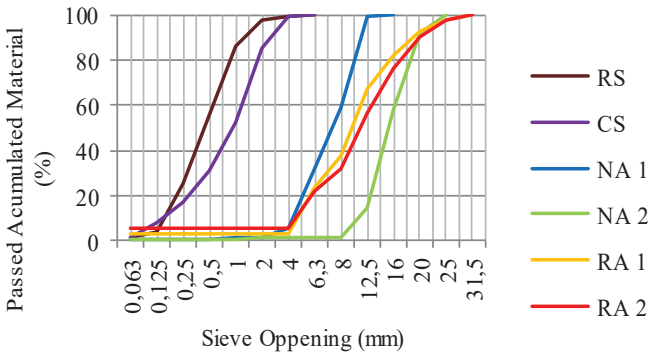

Fig. 1 Aggregate sieve analysis

TABLE I
Recycled Aggregate Constituents

Aggregate/ Constituent	Rc (%)	Ru (%)	Rb (%)	Ra (%)	Rg (%)	X (%)	FL (cm³/kg)
RA1	74.50	21.30	3,57	0.14	0.10	0.40	0.55
RA2	37.26	26.20	34.06	0.08	0.03	2.38	0.62

Ethylene Blue and Sand Equivalent (Table II): The results

show that the RA has higher fines contents and methylene blue values than the NA, particularly RA2, which might be associated to its higher clay content. It can also be concluded that the sand equivalent values follows the same trend than the methylene blue values.

TABLE II
AGGREGATE PROPERTIES

Property/ Aggregate	RS	CS	NA1	NA2	RA1	RA2
Size class	0/2	0/4	4/12.5	12.5/20	4/20	4/20
Fines (%)	1.5	1.8	0.8	0.3	2.9	5.6
Mytilene blue 0/2 (g/Kg)	0.5	0.6	---	---	2.0	6.7
Sand Equivalent 0/2 (%)	79.4	87.9	---	---	36.1	23.7
Shape index (%)	-----	---	15.0	10.0	9.7	24.2
Dry specific density	2.626	2.662	2.648	2.283	2.286	2.162
Saturated specific density	2.631	2.691	2.676	2.696	2.420	2.331
Water absorption (%)	0.2	1.1	1.1	0.5	5.9	7.8
LA (%)	---	---	26.0	35.7	43.3	49.8
Drying shrinkage (%)			0.013		0.031	0.035
Mass Stability (%)			4.6		7.6	8.5

Shape Index (Table II): The shape index of old concrete particles is lower than that of NA but it increases dramatically with the content of ceramic materials. Ceramic elements like bricks, roof, floor or wall tiles, show a much smaller dimension than the other 2, leading to high shape indexes of ceramic RA. The results are in agreement with the reported by others [37], [38].

Specific Density and Water Absorption (Table II): The density of the 4 NA is in the expected range of limestone [38]. Whereas the density of RA is much lower and decreases with the content of ceramic particles. The values are also in the range obtained by others [39], [40]. As expected, the RA shows a higher water absorption capacity than the NA, increasing with the content of ceramic materials, that can be matched to its densities.

Los-Angeles Coefficient (Table II): Los Angeles coefficients of RA are much lower than those of NA and decrease with the ceramic content, which can be related to the density trend. Similar results were found by Vegas et al [41] and Mas et al [36].

Drying Shrinkage and Mass Stability (Table II): The results presented in table 2 show that the reference shrinkage strain is very low, which may be related to the limestone properties [42].The incorporation of RA increases the shrinkage strain dramatically due to a larger pore volume (diameter between 6-30 nm), specific surface area [42] and less stiffness [3], caused by the attached mortar. In the same way, drying shrinkage strain grows with the content of ceramic particles, which could be also related to the higher clay content [43]. Drying shrinkage is proportional to the mass stability which follows the water absorption trend.

IV. CONCRETE TEST PROGRAM

A. Mix Compositions

The compositions were calculated by following Faury´s method. The cement and water content was adjusted experimentally with the goal to reach an initial slump of 130±20 mm, corresponding to the workability class S3 [44]. The water absorption was compensate with extra water. The amount used was chosen so that about 80% of the aggregate absorption capacity is reached. A staged mixing approach was followed [45] to reach 80% pre-saturation of the aggregates before introducing the binder. One reference mix with NA (NAC) only, and 2 mixes with different types RA, labeled RA1C and RA2C were prepared. The effective W/C ratio is 0.6 in all mixes and the binder is a CEM II 32.5. The mix compositions are presented in Table III.

B. Workability

Workability was evaluated by the slump test according to NP EN 12350-2 [46]. The first reading was executed after finish the mix and the following readings were taken every 30 min for 3 hours. Between measurements the fresh concrete stayed in the stopped mixer, before each test the mixer was turned on for about 20 s to break the concrete bonds.

TABLE III
CONCRETE MIX COMPOSITIONS

Materials/Mix	NAC	RA1C	RA2C
RS (Kg/ m³)	289	261	250
CS (Kg/ m³)	343	310	297
NA1 (Kg/ m³)	523	0	0
NA2 (Kg/ m³)	649	0	0
RA1 or 2 or 3 (Kg/ m³)	0	1059	1018
CEM II 32,5 (Kg/ m³)	350	350	350
Water (l/ m³)	210	210	210
Extra Water (l/ m³)	9.52	51.98	69.83

C. Setting Time

A test was performed to determine the initial and final setting times by adapting the NP 1387 [47]. The mold was filled to the top to ensure that the wind blows over the concrete surface. The filled mold was not sealed and it was exposed to a 30±1°C temperature, 50±1% relative humidity in a wind tunnel with air velocity of 6 m/s. The curing conditions were the same as the used in the cracking tests. The readings were taken every 30 minutes after the beginning of hydration and until the final set was reached.

D. Evaporation

Water evaporation tests were performed for all mixes. The molds were 80 mm high and 150 mm large, having the same dimensions as the cracking rings. After casting, the specimens were placed in the wind tunnel together with the restricted shrinkage samples. The weight loss was measured every 30 minutes for 6 hours. The evaporation rate was calculated by dividing the mass loss in Kg through the exposed area.
A second evaporation test was performed with water only, to measure the free water evaporation rate.

E. Bleeding

For the bleeding tests a cube with an edge of 15 cm up to a high of 8 cm was filled to ensure the same dimensions as those of the cracking equipment. The specimens were covered with a glass and placed in the same room as the cracking test. The

bleeding water was taken from the specimen with a plastic pipette and weighted on a high precision balance.

F. Cracking Test

Cracking was evaluated using the Dahl's ring test. The ring had an inner and outer radius of 290 and 600 mm, respectively. The concrete ring was 150 mm thick and 80 mm high. The steel walls of the equipment were 5 mm thick. Twelve steel webs penetrating 30 mm into the sample over the full depth, were equip-spaced around the circumference of the outer ring acting as crack inducers. The concrete was cast between the inner and outer steel ring and then the samples were placed in the wind tunnel (Fig. 2) for 6 hours. Two specimens were prepared for each mix composition. After 6 hours the cracks were photographed and the scaled photos were introduced into a AutoCAD program to evaluate the cracks. The total crack area was measured , the total crack length, the maximum crack opening and the average crack opening.

Fig. 2 Cracking specimens in the wind tunnel

V. Results and Discussion

A. Workability

Fig. 3 clearly shows that the ITZ water flow from the RA is nearly suppressed, the swelling after 30 min is almost negligible. The slump decrease is nearly linear and the workability changes on time follow the same pattern indicating that there is no water absorption from the aggregates. Whereas the NAC had a large swelling indicating that water flows from the 80% pre-saturated NA to the engaging cement paste.

Fig. 3 also shows that the NAC has a higher slump peak and a larger "S3" period than RA, but after 120 minutes the slump of all mixes became very similar. The initial mixing water was the same for all compositions; the somewhat lower slump of the RAC is due to the higher surface roughness, shape index and the undesirable water flow explained previously. After 120 min the effect of the NA water loss relieves, lowering the initial slump differences between the mixes.

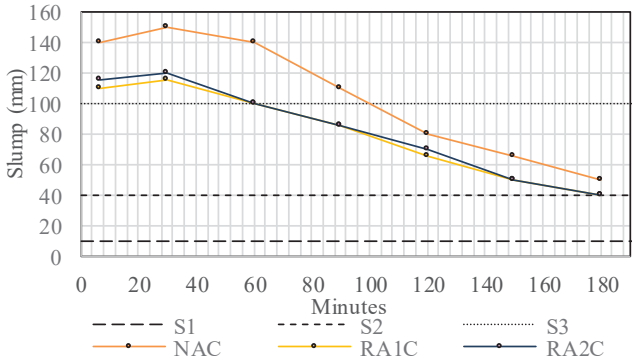

Fig. 3 Slump test

B. Setting Time

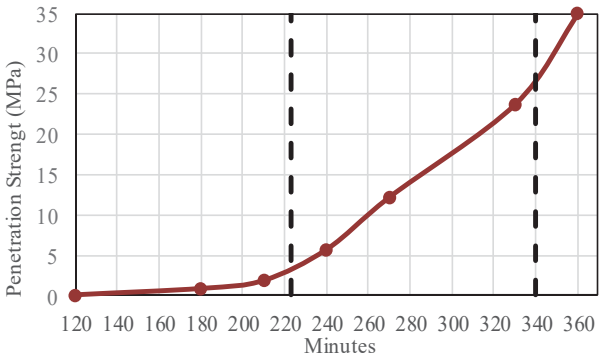

Fig. 4 Setting times

Fig. 4 shows that the initial setting time was reached after 223 minutes and the final set, after 340 minutes. The period between initial and final set was of 117 minutes. The aggregates were pre-saturated to 80% before introducing the binder in the mixture, using a staged mixing approach. It was assumed that the effective w/c ratio (0.6) was the same for all mixes and the setting times too. According to Boschoff and Combrinck [14] the results can be analyzed in the following way: The concrete plastic shrinkage gets isotropic, settlement and bleeding stops at the time of 223 minutes. Before 223 minutes the evaporation rate gets faster than the bleeding rate (drying time). Between the drying time and initial set, capillary pressure reaches its maximum followed by air entry and dropping to zero. After 223 minutes cracking begins and is followed by a progressive increase of the crack opening during 117 minutes. Before 340 minutes PShC cracking stops and drying shrinkage takes place. The development of the stiffness can be related to the development of penetration strength (Fig. 4). Before 223 minutes the concrete was quasi liquid and no stress was built up by the plastic shrinkage strain. In this period, rearrangement of the concrete particles, caused by the gravitational force, transforms the horizontal volume decrease into settlement. At the age of 223 minutes the penetration strength reached 3.5 MPa and the microstructure turned stiff enough to cause horizontal deformation. Due to the restraint introduced by the steel ring and webs, the shrinkage developed stress levels higher than the tensile strength and cracking occurred. In the 117 minutes after initial

set, the volume decrease caused by plastic shrinkage, increased the crack area by growing the crack width. After 340 minutes the concrete microstructure turned too stiff for the occurrence of plastic shrinkage.

C. Bleeding

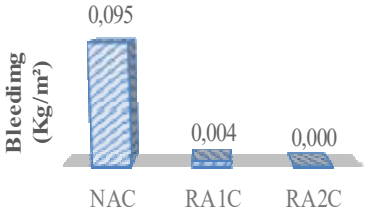

Fig. 5 Bleeding test results

The reference mix (NAC) and RA1C had a bleeding of 0.095 and 0.004 kg/m² respectively, after two hours, but afterwards no more bleeding was observed. No bleeding was detected by RA2C between the end of sample preparation and the end of the testing procedure (6 hours). This result can be explained by the workability test seen before. Water flows from the 80% pre-saturated NA, through the engaging cement paste matrix, to the concrete surface. Another reason could be the large differences between the densities of NA, cement paste and water. This can lead to a gravitational separation of the concrete phases. Similar behavior was not observed for RA mixes, indicating that concrete prepared using this type of aggregates has a higher segregation stability. Bleeding tests indicate that NAC has higher plastic shrinkage settlement than RAC because this phenomenon is proportional to the amount of bleeding water. However, RAC has a higher PShC probability because the bleeding water delays the capillary pressure. Nevertheless the bleeding water is in a very small amount in comparison with the evaporation water (see evaporation). Moreover it blows away when subjected to wind. Thus, the bleeding water should not influence the cracking PShC significantly. Bleeding didn't occurred up to the initial setting time as described by Boschoff and Combrinck [14] indicating that the bleeding time must depend on the mix composition.

D. Evaporation

Fig. 6 shows that the evaporation rate of all mixes is nearly the same. In the first two hours NAC had a somewhat higher evaporation than RA1C whereas RA2C had a somewhat lower rate than RA1C. This may be associated to the bleeding explained before. This behavior seems to increase with the content of ceramic particles.

The free water evaporation rate was 1.4 Kg/m² per hour and the evaporation rate from the concrete surface, in the first hours, was about 1.2 Kg/m² per hour. This is considered a propitious climate for PShC occurrence. It is recommended that when the evaporation rate from fresh concrete approaches 1.0 Kg/m² per hour precautions against PShC are necessary [7].

E. Mass Loss Before Initial Set

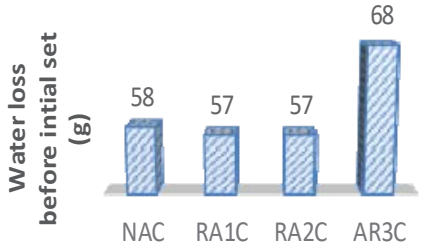

Fig. 6 Evaporation test results

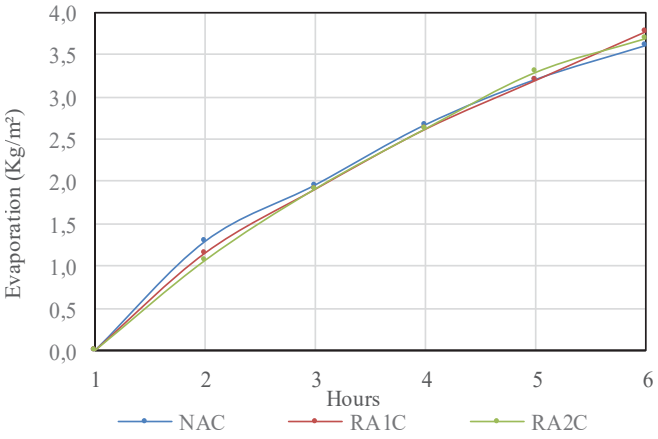

Fig. 7 Amount of water evaporated before initial setting time

The cracking area is proportional to the amount of water lost before initial setting time [18]. Fig. 7 shows that NAC loses 1 g water more that AR1C and AR2C, which is in agreement with the results of the evaporation test.

TABLE IV
PLASTIC SHRINKAGE CRACKING

Mix	Number of Cracks (Unit)	Crack area (mm²)	Crack length (mm)	Maximum crack width (mm)	Average crack width (mm)
NAC	5.5	34	350	0.31	0.10
RA1C	4	30	272	0.29	0.11
RA2C	3.5	29	217	0.40	0.13

F. Plastic Shrinkage Cracking

Table IV shows that the number of cracks, the crack area and crack length follows the same trend. RA1C cracked less than the reference mix whereas RA2C cracked less than RA1C. This trend can easily be linked to the amount of water lost before initial set and to the evaporation rate. Cracking (Fig. 8) increased with the amount of water evaporated before initial set and with the evaporation rate in the first two hours. Comparing RA1C and RA2C it can be observed that they lost the same amount of water before initial setting time but the evaporation rate had a somewhat different evolution. RA1C had a higher evaporation rate in the first two hours and RA2C had a higher rate in the last two hours before initial set was reached. Since RA1C cracked more that RA2C it can be concluded that the early evaporation, when the concrete microstructure is less stiff, has a stronger effect. NAC follows

the same trend indicating that settlement may have a significant influence on PShC. In the first two hours the concrete is quasi liquid and shrinkage is heterotrophic.

Fig. 8 Example of plastic shrinkage cracking

From the type of aggregates and cracking behavior it can be seen that a higher water absorption reduces the evaporation rate in the firs 2 hours and thus setlement is reduced and PShC too. Fig. 6 shows that in the last 2 hours, before final set, RAC has a higher evaporation rate than NAC. From this behavior it can be deduced that, at this stage, the 80% pre-saturated RA provides internal curing [22], reducing the progressive development of PChC. A lower aggregate density (Table 2) may also reduce the concrete segregation in its fresh state, reducing PShC even more. The same can be associated to the degree of restraint. A lower agregate density and Los Angeles coeficient indicates a lower agreggate stifeness leading to a lower degree of internal restrain. This phenomenom decreases the residual stress cuased by palstic shrinkage strain, acording to Hooks Law, $\sigma = \epsilon E$. Finally, a higher surface rougness and a lower water flow from the 80% pre-saturated RA improves the bond strenght between the agregates and the engaging cement paste matrix.

The maximum crack width is a located phenomenom and may depend on the circumstanteces of the location of each crack. The refered circumstances may be related to the configuration of the corase aggregates relative to the amount mortar and the external restiction of the molds. This property can hardly be related to the mix compositions. Nevertheless, the maximum crack openning increases with the shape index (Table II).

The average crack width is higher in RAC than in NAC and grows with the percentage of ceramic material. A correlation with the evaporation rate or the amount of evaporated water was not found. This result could be related with the shrinkage of the aggregates (Table II). The average crack thickness grows with the shrinkage strain of the aggregtes. In turn, the aggregte shrinkage strain is inversaly proprotional to the aggregate density and proportional to it LA coeficcient.

From the discusion above it can be mentioned that the RAC PShC is somewhat lower than that of NAC so there is no need for aplaying more prevention means than for NAC. The results of these paper correspond to RAC using a staged mixing approach to compensate the aggregte water absorption. When other methods are used to compensate the aggregate water absorption the test results can differ.

VI. Conclusion

RAC cracked less than NAC contrary to what was expected. The staged mixing approach used in this work seems to be a perfect mean to reduce PShC in RAC. In the quasi liquid state it reduces bleeding and settlement to. Moreover in the rigid state it provides internal curing reducing the PShC evolution.

NAC shows much more bleeding water than RAC. Consequently, RAC has lower segregation and settlement. The bleeding of the studied mixes stopped before the initial setting time was reached unlike the reported by others [14].

The evaporation rate of NAC and RAC and are nearly the same. In the first 2 hours RAC evaporated somewhat less than NAC but in the last 2 hours this trend inverts. The amount of cerâmic paticles increases this effect iven more. The amount of evaporated water, before initial set, is somewhat higher in NAC than in RAC, but no differences between the types of RA were observed.

The evaporation rate in the first two hours is the main factor influencig PShC. Consequently RAC cracks less than NAC and the severity of cracking decreases with the amount of ceramic content.

The differences in the evaporation rate in the first two hours can be related to the aggregate density, water absorption and even to the water flow from the 80% saturated agregates to the engaging cement paste. This early eavaporation may be influenced by the concrete segregation stability. A better bond strength and a lower degree of restraint seem to influence positively PShC of RAC.

The number of cracks, the crack area and the crack length follows the same trend. The mentioned properies are proprotional to the evaporation rate in the first two hours. The average crack width is proportional to the agregate shrinkage strain, but cant be related with the evaporation rate.

Craccking of RAC is somewhat less than that of NAC and there is no need to aply more PShC prevention methods than in NAC. Further studies need to be performed in order to evaluate if the PShC behavior of RAC is the same when the aggregate water absorption is campensated by following other methods.

Acknowledgments

Financial support from the European Regional Development Fund, via Algarve Operational Program, grant QREN 30307_Multivalor and from the Luso-American Development Foundation is gratefully acknowledged.

References

[1] A. Sivakumar and M. Santhanam, "A quantitative study on the plastic shrinkage cracking in high strength hybrid fibre reinforced concrete," Cement & Concrete Composites , vol. 29 , p. 575–581, 2007.

[2] A. Almusallam, M. Maslehuddin, M. Abdul-Waris and M. Khan, "Effect of mix proportions on plastic shrinkage cracking of concrete in hot environments," Construction and Building Materials, vol. 12, pp. 353-358, 1998.

[3] M. Eckert, Avaliação da Influência da Retração Inicial no Controlo da Fissuração dos Betões, Escola de Ciências e Tecnologia, Universidade de Évora, Évora: Universidade de Évora, 2014.

[4] P. Lura, B. Pease, G. B. Mazzotta, F. Rajabipour and J. Weiss, "Influence of Shrinkage-Reducing Admixtures on Development of

Plastic Shrinkage Cracks," ACI Materials Journal, Technical Paper, Vols. 104-M22, 2007.
[5] Pihlajavaara and S.E., A review of the main results of a research on the aging phenomena of concrete: Effect of moisture conditions on strength,shrinkage and creep of mature concrete. Cement Concrete Res., 4(5), 1974, p. 761–71.
[6] F. H. Wittmann, "On the Action of Capillary Pressure on Fresh Concrete,," Cement and Concrete Research , Vols. 6, No. 1, pp. 49-56, 1976.
[7] I. Soroka, "Early Volume Changes and Cracking," in Concrete in Hot Environments, National Building Research Institute,Faculty of Civil Engineering,Technion—Israel Institute of Technology, Haifa, Israel, E & FN SPON, 1993, pp. 101-117.
[8] B. Klemczak and A. Knoppik-Wróbel, Early age thermal and shrinkage cracks in concrete structures- influences of geometry and dimensions of a structutre, Poland, 2011.
[9] P. G. Simpkins, D. W. Johnson and D. A. Fleming, "Drying Behavior of Colloidal Silica Gels," Journal of the American Ceramic Society, Vols. 72, No. 10, pp. 1816-1821, 1986.
[10] A. Bentur, Terminology And Definitions in Early Age Cracking in Cementitious Systems ; RILEM TC 181-EAS – Final Report, Technion, Israel Institute of Technology: RILM Puplications S.A.R.L, July 2002, pp. 13-17.
[11] Neville and A.M., Properties of Concrete; 4th Edition, 1995.
[12] Buil and L.M., Contribuition a l`étude du retrait de la pâte de ciment durcissante, Ecole Nationale des Ponts et chaussées, Paris, 1979, p. 67.
[13] Barcelo and e. al, Early Age Shrinkage of concrte: back to the physical mechanisms, UEF conference in Advances in Concrete and Cement, Canada: Mt-Tremblant, August 2000.
[14] W. P. Boshoff and R. Combrinck, "Modelling the severity of plastic shrinkage cracking in concrete," Cement and Concrete Research, vol. 48, p. 34–39, 2013.
[15] R. Combrinck, "Plastic shrinkage cracking in conventional and low volume fibre reinforced concrete, , 2011, Stellenbosch University, South Africa.," MSc Thesis, 2011.
[16] A. Boumiz, Etude comparée des évolutions mecaniques et chimiques de pâte de ciment et mortiers a tres jeune age, PhD-thesis of Univerité Paris 7, 1995.
[17] B. L., S. Boivin, S. Rigaud, P. Acker, P. Clauvaud and C. Boulay, Linear vs Volumetric Autogeneous Shrinkage Measurements: Material Behavior or Experimental Artifact , ref 3, pp. 109-126.
[18] A. Radocea, "A model of plastic shrinkage," Mag. Concr. Res, vol. 46 , p. 125–132, 1994.
[19] A. Leemann, P. Nygaard and P. Lura, "Impact of admixtures on the plastic shrinkage cracking," Cement & Concrete Composites, vol. 46, pp. 1-7, 2014.
[20] J. Mora-Ruacho, R. Gettu and A. Aguado, "Influence of shrinkage-reducing admixtures on the reduction of plastic shrinkage cracking in concrete," Cement and Concrete Research, vol. 39, p. 141–146, 2009.
[21] J. Saliba, E. Rozière, F. Grondin, and A. Loukili, "Influence of shrinkage-reducing admixtures on plastic and long-term shrinkage," Cement & Concrete Composites , vol. 33, p. 209–217, 2011.
[22] A. Leemann , P. Lura and R. Bolliger , "Internes Curing für den Beton (in German).," Baublatt, 2011.
[23] J. Branch, A. Rawling and D. Hannant, "The effects of fibers on the plastic shrinkage cracking of high strength concrete," Material and Structures, vol. 35, pp. 189-194, 2002.
[24] N. Banthia and R. Gupta, "Influence of polypropylene fiber geometry on plastic shrinkage cracking in concrete," Cement and Concrete Research , vol. 36 , p. 1263 – 1267, 2006.
[25] O. S. Baghabra Al-Amoudi, T. O. Abiola and M. Maslehuddin, "Effect of superplasticizer on plastic shrinkage of plain and silica fume cement concretes," Construction and Building Materials, vol. 20, p. 642–647, 2006 .
[26] D. Ravina and R. Shalon, Shrinkage of fresh mortars cast under and exposed to hot dry climate conditions. In Proc. RILEM/CEMBUREAU Colloq. on Shrinkage of Hydraulic Concretes; Vol. II, Edigrafis, Madrid, 1961.
[27] N. E. 9.-1. 2011, Ensaios das propriedades geométricas dos agregados. Parte 11: Ensaio para classificação dos constituintes de agregados grossos reciclados, 20011.
[28] NP EN 933-1, Ensaios das propriedades geométricas dos agregados. Parte 1: Análise granulométrica, Método de peneiração, IPQ, 2000.
[29] NP EN 12620, Agregados para betão, IPQ, 2004.
[30] NP EN 933-9, Ensaios das propiedades geométricas dos agregados, Parte 9: Determinação do teor de finos, Ensaio do azul de metileno, IPQ, 2002.
[31] NP EN 933-8, Ensaios das propriedades geométricas dos agregados, Parte 8: Determinação do teor de finos, Equivalente de areia, IPQ, 2002.
[32] NP EN 933-4, Ensaios das propriedades geométricas dos agregados, Parte 4: Determinação da forma das partículas-Índice de Forma.
[33] NP EN 1097-2, Ensaios das propriedades mecânicas e físicas dos agregados, Parte 2: Método para a determinação da resistência à fragmentação, 2002.
[34] 1-4. N. EN, nsaios das propriedades térmicas e de meteorização dos agregados. Parte 4: Determinação da retração por secagem, IPQ, 2002.
[35] J. Yang, Q. Du and Y. Bao, "Concrete with recycled concrete aggregate and crushed clay bricks," Construction and Building Materials , vol. 25, pp. 1935-1945, 2011.
[36] B. Mas, A. Cladera, T. del Olmo and F. Pitarch, Influence of the amount of mixed recycled aggregates on the properties of concrete for non-structural use, Construction and Building Materials 27, 2012, pp. 612-622.
[37] D. Matias, J. de Brito, A. Rosa and D. Pedro, Mechanical properties of concrete produced with recycled coarse aggregates – Influence of the use of superplasticizers, Construction and Building Materials 44, 2013, pp. 101-109.
[38] P. B. Cachim, Mechanical properties of brick aggregate concrete,Construction and Building Materials 23, 2009, p. 1292–1297.
[39] C. S. Poon and D. Chan, Feasible use of recycled concrete aggregates and crushed clay brick as unbound road sub-base Construction and Building Materials 20, 2006, p. 578–585.
[40] J. Yang, Q. Du and Y. Bao, Concrete with recycled concrete aggregate and crushed clay bricks,Construction and Building Materials 25, 2011, pp. 1935-1945.
[41] I. Vegas, J. Ibañez, A. Lisbona and A. Sáez de Cortazar, Pre-normative research on the use of mixed recycled aggregates in unbound road sections. Constr Build Mater, 2011.
[42] W. Zhang, M. Zakaria and Y. Hama, "Influence of aggregate materials characteristics on the drying shrinkage properties of mortar and concrete," Construction and Building Materials, vol. 49, p. 500–510, 2013.
[43] R. Smith and L. Collis, Aggregates, sand, gravel and crushed rock aggregates for construction purposes, 3 (Special Edition) ed., vol. 17, Geological Society.
[44] NP EN 206-1, Betão. Parte 1: Especificação, produção e conformidade.
[45] M. Eckert and M. Oliveira, "Mitigation of the negative effects of recycledt aggregate water absorption in concrete technology," XVII. ERMCO Congress, 2015.
[46] NP EN 12350-2, Ensaios do betão fresco, Parte 2: Ensaios de abaixamento, Portugal: IPQ, 2002.
[47] NP-1387, Determinação dos dempos de presa, 1976.